Dalton Transactions

ROYAL SOCIETY OF CHEMISTRY

PAPER

View Article Online
View Journal | View Issue

Cite this: *Dalton Trans.*, 2021, **50**, 11243

Spin transition triggered by desorption of crystal solvents for a two-dimensional cobalt(II) complex with hydrogen bonding†

Takuya Kanetomo, * Kiwamu Inokuma, Yuya Naoi and Masaya Enomoto

Received 13th June 2021,
Accepted 16th July 2021

DOI: 10.1039/d1dt01934a

rsc.li/dalton

$[Co(5tpybNOH)_2](BPh_4)_2$ (**1**; 5tpybNOH = 5,5″-bis(*N*-*tert*-butyl hydroxylamino)-2,2′:6′,2″-terpyridine) has a two-dimensional (2D) structure through a hydrogen bond between the NOH sites, as revealed by X-ray crystallography. The crystal solvents were desorbed above 300 K as shown by thermal analyses and powder X-ray crystallography. The removal of the crystal solvents allowed irreversible structural changes and a spin transition of the Co centre from S = 1/2 to 3/2.

Introduction

The spin crossover (SCO) phenomenon is a reversible spin transition based on the difference in the spin configuration of a metal centre caused by external stimuli.[1] The SCO-active materials have been applied to the development of switches, sensors and memory devices.[2,3] To obtain a beneficial magnetic-switching material, it is necessary to enhance the cooperativity between the SCO units. Molecular design with intermolecular hydrogen bonding is an effective approach to obtain high cooperativity because of its high directivity and strong intermolecular interaction compared to other non-covalent contacts such as π–π interactions.[4–7]

A cobalt(II) complex can exhibit SCO behaviour between the high-spin (HS; S = 3/2) and low-spin (LS; S = 1/2) states with a small difference in entropy. The compound 2,2′:6′,2″-terpyridine (terpy, Fig. 1a) has been utilised as a ligand and has contributed to the SCO behaviour in the Co^{2+} ion.[8–11] In addition, a variety of functional groups (R = hydroxy,[12–14] alkoxy,[15,16] pyridyl[17,18] and others[19–23]) may be easily introduced at the 4′-position of the terpy ligand. This chemical modification allows the Co-terpy complexes to control the molecular and crystal structures. However, in previous studies of the Co-SCO complexes, there have been no reports on the terpy ligand being chemically modified at positions other than the 4′-position.

In this study, we focused on the introduction of substituents at the 5,5″-positions of the terpy molecule and prepared a terpy analogue, 5,5″-bis(*N*-*tert*-butyl hydroxylamino)-2,2′:6′,2″-terpyridine (5tpybNOH, Fig. 1b). The chemical modification at the 5,5″-positions allows the formation of a 2D network along two terpy ligands because the $[Co(terpy)_2]^{2+}$ unit has a cross-like structure. In addition, the insertion of the hydroxylamine group (>N–OH) is expected to provide an intermolecular hydrogen bond through the NOH sites. A novel cobalt(II) complex $[Co(5tpybNOH)_2](BPh_4)_2$ (**1**; BPh_4 = tetraphenyl borate) was synthesised and it showed intermolecular contact through the NOH sites. Crystallisation solvents (acetone and water molecules) were present in the void spaces. The solvents can be easily desorbed above 300 K, and simultaneously, the desorption can result in a structural change and spin transition.

Experimental

Materials and methods

Tetrahydrofuran (THF) was used after distillation from sodium/benzophenone under N_2 gas. Other solvents were purchased and used without further purification. ^{1}H and ^{13}C NMR experiments (400 and 100 MHz, respectively) were performed in DMSO-d_6 on an ECZ400S spectrometer (JEOL). The chemical shifts (given in ppm) were measured *versus* the central peak of DMSO (^{1}H NMR: 2.50 ppm and ^{13}C NMR: 39.52 ppm) as a reference.[24] The splitting patterns are designated as follows: s (singlet), d (doublet), t (triplet), dd (doublet

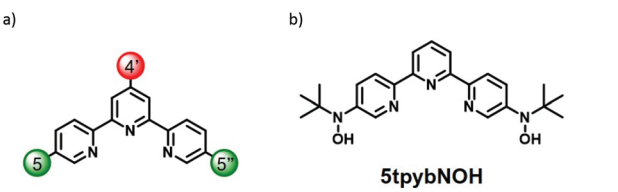

Fig. 1 Structural formulas of (a) tpy and (b) 5tpybNOH.

Department of Chemistry, Faculty of Science Division 1, Tokyo University of Science, 1-3 Kagurazaka, Shinjuku-kuTokyo 162-8601, Japan. E-mail: kanetomo@rs.tus.ac.jp

†CCDC 2087500. For crystallographic data in CIF or other electronic format see DOI: 10.1039/d1dt01934a.

of doublets) and m (multiplet). Infrared (IR) spectra were obtained on an FT/IR-4600 (Jasco) spectrometer using a diamond attenuated total reflectance (ATR) method. The spectral data are obtained as major peaks in wavenumbers (cm^{-1}) and recorded in a spectral window of 4000–400 cm^{-1}. Elemental analyses were carried out with a PerkinElmer Series II CHNS/O 2400 analyser. High resolution mass spectra (HRMS) were recorded in an electrospray ionization (ESI) mode using an AccuTOF-JMS-T100LP (JEOL) spectrometer. The specimen was dissolved in methanol. Powder X-ray diffraction (PXRD) spectra were recorded using a Rigaku MiniFlex600 diffractometer (Cu Kα radiation: λ = 1.54184 Å) in the range of 300–430 K. Thermogravimetry (TG) and differential thermal analysis (DTA) of **1** were carried out on a Bruker AXS TG2000SA instrument. The temperature scan rate was 2 K min^{-1} in the range of 296–481 K. Differential scanning calorimetry (DSC) was performed on a Bruker DSC3200A apparatus. The temperature scan rate was 5 K min^{-1}.

Synthesis

Synthesis of 5,5″-bis(*N*-*tert*-butyl hydroxylamino)-2,2′:6′,2″-terpyridine (5tpybNOH). An *n*-hexane solution of *n*-BuLi (1.57 mol L^{-1}, 4.0 mL, 6.3 mmol) was added dropwise to a THF solution (30 mL) of 5,5″-dibromo-2,2′:6′,2″-terpyridine (1.13 g, 2.89 mmol)[25] with a syringe below −100 °C. The mixture was stirred for 0.5 h, and a THF solution (20 mL) of 2-methyl-2-nitrosopropane (0.85 g, 14.3 mmol) was added using a dropping funnel. The mixture was stirred for 1 h and spontaneously warmed up to room temperature for 1 h. After the reaction was quenched with a saturated NH_4Cl aqueous solution, the mixture was neutralized with a saturated $NaHCO_3$ aqueous solution. The organic layer extracted with $CHCl_3$ was dried over anhydrous $MgSO_4$. The filtrate was concentrated under reduced pressure, and the crude product was purified by recrystallization with CH_2Cl_2, affording a colourless powder of 375.2 mg (2.89 mmol, 31%). Mp. 205 °C (decomp.). ^{1}H NMR (400 MHz, DMSO-d_6): δ 8.64 (s, 2H), 8.53–8.51 (m, 4H), 8.34 (d, J = 7.8 Hz, 2H), 8.03 (t, J = 7.8 Hz, 1H), 7.82 (dd, J = 8.2 Hz, J' = 2.7 Hz, 2H) and 1.15 (s, 18H). ^{13}C NMR (100 MHz, DMSO-d_6): δ 154.7, 150.7, 147.4, 144.8, 138.2, 131.9, 119.8, 119.7, 60.15 and 25.91. IR (ATR): 1447, 1361, 1197, 818, 756, 653, 617, 573, 553 and 412 cm^{-1}. HRMS (ESI+): m/z calcd for $C_{23}H_{30}N_5O_2$ $[M + H]^+$: 408.23995, found: 408.24279.

Synthesis of $[Co(5tpybNOH)_2](BPh_4)_2(C_3H_6O)_{2.5}(H_2O)_{3.3}$ ($\mathbf{1}\cdot(C_3H_6O)_{2.5}(H_2O)_{3.3}$). $CoCl_2\cdot 6H_2O$ (23.8 mg, 0.100 mmol) and 5tpybNOH (82.9 mg, 0.203 mmol) were dissolved in MeOH (15 mL). The mixture was stirred for 5 minutes. After $NaBPh_4$ as a powder (68.5 mg, 0.200 mmol) was added to the solution, a brown powder was collected and dried over air. The product was purified by recrystallization *via* a vapor diffusion approach with acetone and *n*-hexane, affording black crystals of 46.0 mg (0.0268 mmol, 26%). Anal. calcd for $C_{101.5}H_{119.6}B_2CoN_{10}O_{9.8}$: C, 71.00; H, 7.02; N, 8.16%. Found: C, 71.18; H, 6.70; N, 7.98%. IR (ATR): 3447, 2974, 1559, 1447, 1183, 1030, 813, 731, 703 and 611 cm^{-1}.

Single crystal X-ray diffraction (SXRD)

The X-ray diffraction data of $\mathbf{1}\cdot C_3H_6O_5$ were collected on a Rigaku XtaLAB Synergy-S diffractometer (Cu Kα radiation: λ = 1.54184 Å). X-ray data analyses were carried out using the SHELXT[26] and SHELXL[27] programs operated with the Olex2 interface.[28] A numerical absorption correction was applied. All the hydrogen atoms were refined as "riding". The thermal displacement parameters of the non-hydrogen atoms were refined anisotropically. The contribution of the disordered solvent was removed using the SQUEEZE option from PLATON operated with the Olex2 interface.[28] The CCDC number is 2087500.†

Magnetic measurements

The direct current (dc) magnetic susceptibility of **1** was measured on a Quantum Design MPMS-XL7 SQUID magnetometer equipped with a 7 T coil in the temperature range of 2–400 K. The magnetic data were corrected using diamagnetic blank data of the sample holder measured separately. The diamagnetic contribution of the sample itself was estimated from Pascal's constant.[29]

Results and discussion

Synthesis and characterization

The terpyridine-based bishydroxylamine ligand 5tpybNOH was prepared using 5,5″-dibromo-2,2′:6′,2″-terpyridine *via* the conventional organolithium method. After complexation between $CoCl_2\cdot 6H_2O$, 5tpybNOH and $NaBPh_4$ in methanol, the product was purified by recrystallisation *via* the vapour diffusion approach with acetone and *n*-hexane, affording black crystals of **1**. For elemental analysis, the experimental values agreed with the calculated values, including 2.5 acetone and 3.3 water molecules ($\mathbf{1}\cdot(C_3H_6O)_{2.5}(H_2O)_{3.3}$) after collection and immediate measurement. The presence of solvents was also confirmed by thermal and X-ray crystallographic analyses (for details, see below).

Single-crystal X-ray crystallography

The crystal structure of **1** was determined by SXRD measurement at 100 K, as shown in Fig. 2 and Table 1. There are a $[Co(5tpybNOH)_2]$ dication, two BPh_4 anions and an acetone molecule as a crystallographically independent molecule in a unit cell. In addition, disordered solvent molecules, which were accounted for in the SQUEEZE program operated using the Olex2 interface, are present.[28] The Co^{2+} centre was 6-coordinated with two 5tpybNOH ligands, giving the N_6 coordination environment. The Co1–N2 and –N7 bond lengths of 1.892(9) and 1.912(9) Å, respectively, are smaller than the other Co–N bond lengths of 2.053(8)–2.070(9) Å. These findings suggest that the N2 and N7 atoms are located at the axial positions around the Co^{2+} ion, and the coordination polyhedra have a suppressed octahedral geometry along the N2, Co1 and N7 atoms. The mean of the Co–N bond lengths (d_{mean}) and the octahedral distortion parameter (Σ)[9] allowed the prediction of the spin state of the cobalt(II) centre. Fig. 3 shows a plot of the

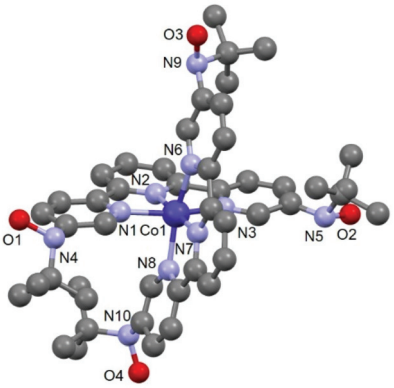

Fig. 2 Molecular structure of the Co(5tpybNOH)$_2$ unit. H atoms and the acetone and BPh$_4$ molecules are omitted for clarity. Only the major configuration of the *N*-*tert*-butyl hydroxylamine groups including N5 and N10 atoms is shown.

Table 1 Selected crystallographic data for **1**·C$_3$H$_6$O

Complex	**1**·C$_3$H$_6$O$_5$
Formula	$C_{97}H_{104}B_2CoN_{10}O_5$
Fw	1570.45
T/K	100
Crystal system	Monoclinic
Space group	*Cc*
a/Å	23.3784(4)
b/Å	19.8247(3)
c/Å	22.6637(4)
β/°	90.025(2)
V/Å^3	10503.9(3)
Z	4
d_{calcd}/g cm^{-3}	0.993
μ(Mo Kα)/mm^{-1}	1.657
$R(F)^a$ ($I > 2\sigma(I)$)	0.0551
$R_w(F^2)^b$ (all data)	0.1446
Goodness of fit	1.060
No. of unique reflns	38333

$^a R = \Sigma||F_o| - |F_c||/\Sigma|F_o|$. $^b R_w = [\Sigma w(|F_o| - |F_c|)^2/\Sigma w|F_o|^2]^{1/2}$.

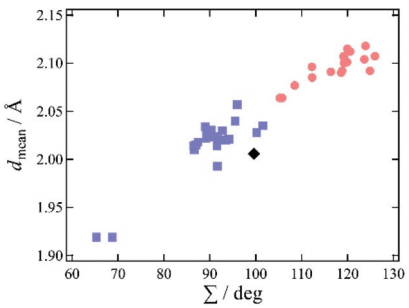

Fig. 3 Plot of the mean of Co–N bond lengths (d_{mean}) against the octahedral distortion parameter Σ. The red circles and blue squares represent the HS and LS states of the Co^{2+} centre, respectively. The black diamond represents the present data.

above two parameters based on the data from previous studies (Table 2).[8–23] Compound **1** at 100 K has a d_{mean} value of 2.006 Å and a Σ value of 99.62°. The data are superimposed in Fig. 3 (black diamond), indicating that the Co centre in **1** is of the LS state.

Table 2 The mean of coordination bonds Co–N (d_{mean}) and the octahedral distortion parameter (Σ) for the HS and LS states of cobalt(II) compounds with the terpyridine-based ligand

Compound[a]	T/K	d_{mean}/Å	Σ/°	Ref.
High-spin state				
[Co(terpy)$_2$](ClO$_4$)$_2$(H$_2$O)$_{0.5}$	243	2.101	119.92	8
[Co(4-terpyridone)$_2$](ClO$_4$)$_2$(H$_2$O)	293	2.085	112.33	12
[Co(4-terpyridone)$_2$](BF$_4$)$_2$(H$_2$O)	293	2.064	105.27	13
[Co(4-terpyridone)$_2$](PF$_6$)	293	2.118	123.92	13
[Co(C14-terpy)$_2$](BF$_4$)$_2$(MeOH)	190	2.106	119.26	16
[Co(4-terpyridone)$_2$](CF$_3$SO$_3$)$_2$(H$_2$O)	293	2.096	112.24	14
[Co(4-terpyridone)$_2$](CF$_3$SO$_3$)$_2$(H$_2$O)	293	2.100	119.27	14
[Co(terpy)$_2$](BF$_4$)$_2$	375	2.115	119.99	9
[Co(pyterpy)$_2$](PF$_6$)$_2$(MeOH)$_2$	250	2.091	116.35	17
[Co(tpyphNO)$_2$](CF$_3$SO$_3$)$_2$	300	2.104	123.66	20
[Co(terpy)$_2$](CF$_3$SO$_3$)$_2$	400	2.092	118.83	20
[Co(Naph-C2-terpy)$_2$](BF$_4$)$_2$(MeOH)$_2$	273	2.064	105.78	21
[Co(Naph-C2-terpy)$_2$](BF$_4$)$_2$	200	2.107	126.00	21
[Co(L)$_2$](BDS)	400	2.092	124.89	22
[Co(COO-terpy)$_2$](H$_2$O)$_4$	420	2.112	120.57	23
[Co(COO-terpy)$_2$]	370	2.107	119.13	23
[Co(terpy)$_2$](BF$_4$)$_2$·H$_2$O	123	2.077	108.48	11
[Co(terpy)$_2$](BF$_4$)$_2$	333	2.090	118.62	11
Low-spin state				
[Co(4-terpyridone)$_2$](BF$_4$)(SiF$_6$)$_{0.5}$(MeOH)	105	2.023	90.31	13
[Co(4-terpyridone)$_2$][Co(NCS)$_4$](MeOH)$_{0.5}$	293	1.919	65.28	13
[Co(4-terpyridone)$_2$](I)$_2$(H$_2$O)$_5$	293	1.919	68.73	13
[Co(C14-terpy)$_2$](BF$_4$)$_2$(MeOH)	10	1.993	91.64	16
[Co(4-terpyridone)$_2$](CF$_3$SO$_3$)$_2$(H$_2$O)	120	2.030	92.78	14
[Co(terpy)$_2$](BF$_4$)$_2$	30	2.034	89.02	9
[Co(terpy)$_2$](BF$_4$)$_2$	100	2.031	90.34	9
[Co(pyterpy)$_2$](PF$_6$)$_2$(MeOH)$_2$	100	2.021	91.72	17
[Co(pyterpy)$_2$](PF$_6$)$_2$(MeOH)(CH$_2$Cl$_2$)$_2$	100	2.014	91.59	17
[Co(Fctpy)$_2$](PF$_6$)$_2$(MeCN)$_2$	100	2.021	94.22	19
[Co(pyterpy)$_2$](TCNQ)$_2$(DMF)(MeOH)	110	2.057	95.97	18
[Co(pyterpy)$_2$](TCNQ)$_2$(MeCN)(MeOH)	110	2.024	90.86	18
[Co(tpyphNO)$_2$](CF$_3$SO$_3$)$_2$	90	2.028	100.22	20
[Co(terpy)$_2$](CF$_3$SO$_3$)$_2$	90	2.020	93.44	20
[Co(Naph-C2-terpy)$_2$](BF$_4$)$_2$(MeOH)$_2$	100	2.022	89.21	21
[Co(Naph-C2-terpy)$_2$](BF$_4$)$_2$	93	2.035	101.56	21
[Co(2-Naph-terpy)$_2$](BF$_4$)$_2$(CHCl$_3$)$_2$	100	2.018	87.42	21
[Co(9-anth-terpy)$_2$](BF$_4$)$_2$(CHCl$_3$)$_{2.5}$	100	2.010	86.57	21
[Co(L)$_2$](BDS)(H$_2$O)$_2$	120	2.015	86.96	22
[Co(L)$_2$](BDS)	120	2.014	86.50	22
[Co(COO-terpy)$_2$](H$_2$O)$_4$	120	2.025	89.22	23
[Co(terpy)$_2$](BF$_4$)$_2$	100	2.040	95.56	11

[a] Terpy = 2,2′:6′,2″-terpyridine; 4-terpyridone = 2,6-bis(2-pyridyl)-4(1*H*)-pyridone; C14-terpy = 4′-tetradecyloxy-2,2′:6′,2″-terpyridine; pyterpy = 4′-(4-pyridyl)-2,2′:6′,2″-terpyridine; tpyphNO = 4′-{4-*tert*-butyl (*N*-oxy) aminophenyl}-2,2′:6′,2″-terpyridine; Naph-C2-terpy = 4′-(2-naphthoxy (ethoxy))-2,2′:6′,2″-terpyridine; L = 4′-(4-bromophenyl)-2,2′:6′,2″-terpyridine; H$_2$BDS = benzene-1,3-disulfonic acid; COOH-terpy = 4′-carboxyl-2,2′:6′,2″-terpyridine; Fctpy = 4′-ferrocenyl-2,2′:6′,2″-terpyridine; 9-anth-terpy = 4′-(9-anthracenyl)-2,2′:6′,2″-terpyridine.

The N–O bond length can provide information on the electronic structure of the NOH site. Three NOH sites, N4–O1, N5–O2 and N9–O3, have N–O bond lengths of 1.432(9), 1.48(2) and 1.447(10) Å, respectively, which are close to those established in previous works (1.451–1.497 Å).[30–35] On the other hand, the N10–O4 bond length of 1.396(15) Å is close to that of a polar-

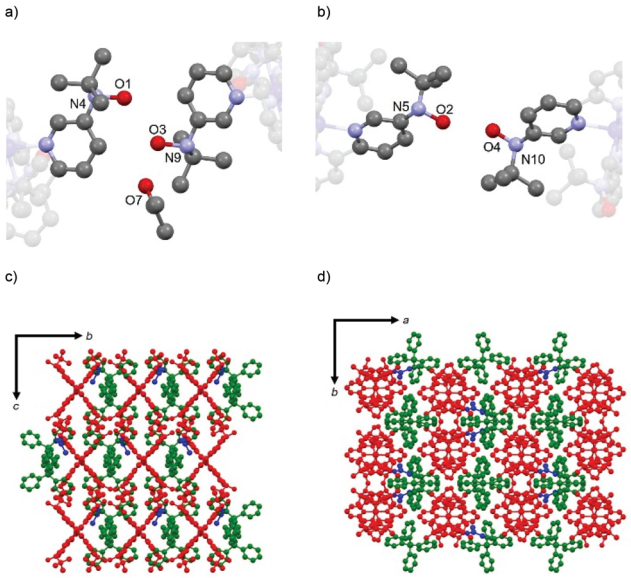

Fig. 4 (a and b) Intermolecular hydrogen bonding between NOH sites. (c and d) Packing of **1** along the (c) *a*- and (d) *c*-axes. Red, green and blue colours represent $Co(5tpybNOH)_2$, BPh_4 and acetone molecules, respectively.

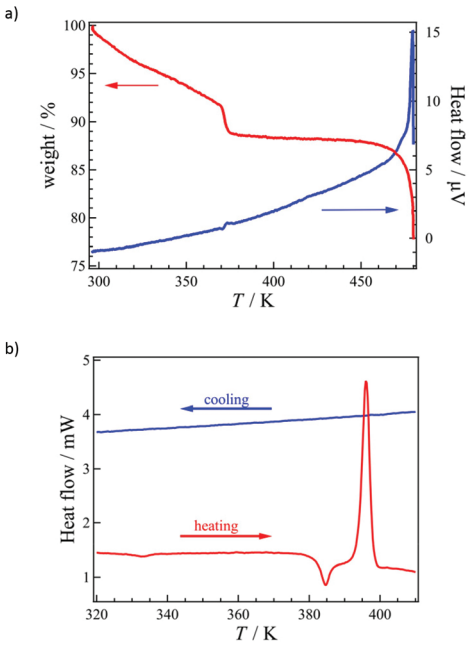

Fig. 5 (a) TG (red) and DTA (blue) and (b) DSC curves for **1**. (b) The red and blue lines represent the heating and cooling processes, respectively.

ized form ($>N^+–O^-$) of 1.4170(15) Å.[36] The polarization at the N10–O4 site could be related to the intermolecular contact. The interatomic O1···O3 and O2···O4 distances as shown in Fig. 4a and b are 3.336 and 2.641 Å, respectively, in which the latter is smaller than the sum of the van der Waals radii (O/O: 3.04 Å).[37] These findings suggest that the O2···O4 contact is strong H-bonding, while the O1···O3 contact is weak. With these intermolecular contacts, **1** formed a 2D structure on the *bc* plane (Fig. 4c). The 2D structure was stacked along the *a*-axis, and a BPh_4 anion was present between these layers. In addition, one acetone molecule as a crystal solvent was located in the void space, and there was a strong intermolecular contact between the acetone and NOH sites (O3···O7: 2.863 Å).

Thermal analyses

To determine the presence of crystal solvents observed in the elemental and X-ray crystallographic analyses, **1** was analyzed by thermogravimetry (TG) and differential thermal analysis (DTA), as shown in Fig. 5a. The TG spectrum showed a gradual decrease from 296 to 370 K. Upon further heating, the TG spectrum showed a sharp drop from 370 to 375 K. Above 375 K, the TG spectrum plateaued at 460 K, and then decreased sharply, indicating decomposition. Here, the decrease upon heating from 296 to 375 K suggests the desorption of all crystallisation solvents of **1**, giving the formula of **1** with no solvents (Fw: 1512.44) in the range of 375–460 K. From this finding, it can be inferred that the change in the weight in the 370–375 K range of approximately 3.3% corresponds to one acetone molecule (Fw: 58.08). Furthermore, the change in the weight at 296–370 K of approximately 8.4% corresponds to 1.5 acetone and 3.3 water molecules (Fw: 146.57). These findings support the formula $\mathbf{1}\cdot(C_3H_6O)_{2.5}(H_2O)_{3.3}$ obtained from the results of elemental analysis. On the other hand, the DTA spectrum showed endothermic and unexpected exothermic peaks at 370–375 K. To understand the details, we performed differential scanning calorimetry (DSC), as shown in Fig. 5b. The red and blue lines represent the heating and cooling processes, respectively. During the heating process, there are two endothermic peaks and one exothermic peak at 330, 385 and 390 K, respectively. The two endothermic peaks suggest the desorption of the solvents (acetone and water molecules) from **1**. On the other hand, the exothermic peak suggests that the irreversible structural change was triggered by the removal of the solvents because there was no peak observed during the cooling process.

Powder X-ray crystallography

We performed the variable-temperature powder X-ray diffraction (VT-PXRD) measurements from 300 K to 430 K, as shown in Fig. 6. The PXRD spectrum at 300 K showed two main peaks at 6.8° and 7.4° (p1 and p2, respectively). The p2 peak remained until 410 K, although p1 decreased upon heating and vanished at 360 K. The findings and the above thermal analyses suggest that the p1 peak corresponds to the simulation from the above SXRD study (black line in Fig. 6), while p2 can be assigned to the desolvated form of **1**. Here, the position of p1 (6.8°) is shifted to lower than that of the strongest peak in the simulation pattern (7.0°) because of the thermal expansion from the difference between temperatures of 100 K for SXRD and 300 K for PXRD measurements. On further heating from 410 K, p2 was broadened, indicating the decomposition of **1**.

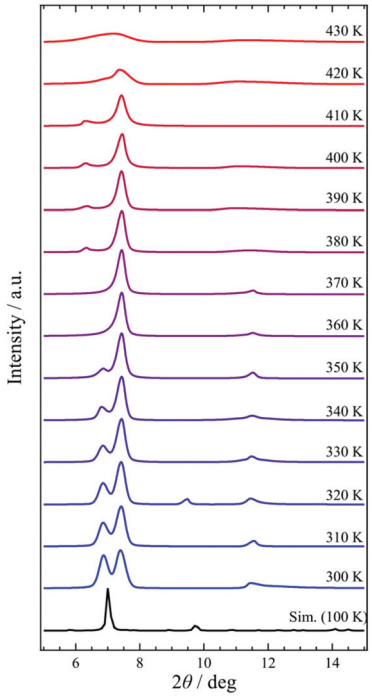

Fig. 6 VT-PXRD measurements of **1** from 300 K to 430 K.

Magnetic properties

The magnetic susceptibility of a polycrystalline specimen of **1**·$(C_3H_6O)_{2.5}(H_2O)_{3.3}$ was measured in the temperature range of 2–400 K, as shown in Fig. 7. During the heating process (red filled circles), the $\chi_m T$ value at 2 K was 0.412 cm^3 K mol^{-1}, which is close to the theoretical value of the LS state for the Co^{2+} ion (S = 1/2 and g = 2.1; $\chi_m T$ = 0.413 cm^3 K mol^{-1}). Upon heating, the $\chi_m T$ value gradually increased from 200 to 310 K owing to the desorption of the disordered acetone and water molecules described in the above SXRD study. On further heating, the $\chi_m T$ value increased sharply and reached 1.88 cm^3 K mol^{-1} at 380 K, which is almost identical to the theoretical value of the HS state for the Co^{2+} ion (S = 3/2 and g = 2.0; $\chi_m T$ = 1.88 cm^3 K mol^{-1}). This spin transition could be triggered by the structural change caused by the desorption of the strongly bound acetone molecule. Upon cooling from 400 to 2 K (blue open squares), the magnetic behaviour showed a difference from that observed during the heating process and the SCO of the Co centre with $T_{1/2}$ = 136 K. In addition, the 2nd heating process from 2 K to 400 K (green filled triangles) showed a similar trend to that of the cooling process. These findings suggest that the desorption of crystal solvents in the 1st heating process caused irreversible structural changes and spin transitions. This was confirmed by the results obtained from the elemental, X-ray crystallographic and thermal analyses.

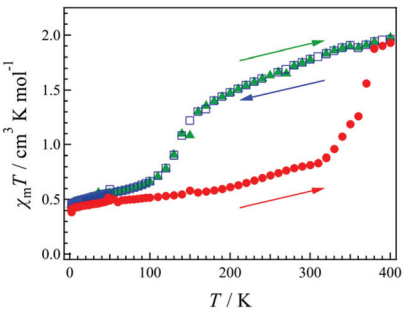

Fig. 7 Temperature dependence of the product $\chi_m T$ measured at 0.5 T for **1**·$(C_3H_6O)_{2.5}(H_2O)_{3.3}$. The red filled circles, blue open squares and green filled triangles represent the 1st heating, cooling and 2nd heating processes, respectively.

Conclusions

In this study, the novel 5,5″-substituted terpyridine ligand 5tpybNOH was utilised for the synthesis of **1**. Compound **1** had a 2D structure through the H-bond between the NOH sites, and there were acetone and water molecules in the void spaces. This was revealed by elemental, X-ray structural and thermal analyses. The DSC and VT-PXRD results suggest that the desorption of acetone caused irreversible structural changes and spin transitions. In addition, **1**, in the absence of crystal solvents, showed SCO behaviour with $T_{1/2}$ = 136 K during the cooling process. This study confirms the valuable role of the hydroxylamine group and the substitution at the 5,5″-positions of the terpy ligand in the Co-SCO compounds.

Conflicts of interest

There are no conflicts to declare.

Acknowledgements

This study was financially supported by KAKENHI (JSPS/21K14604). We acknowledge Mr Hiroyasu Sato and Mr Akihito Yamano (Rigaku Co.) for refinement of the SXRD data of **1**.

Notes and references

1 *Spin Crossover in Transition Metal Compounds I, II and III*, ed. P. Gütlich and H. A. Goodwin, Springer, Berlin, Germany, 2004.
2 O. Sato, *Nat. Chem.*, 2016, **8**, 644.
3 M. Feng, Z.-Y. Ruan, Y.-C. Chen and M.-L. Tong, *Chem. Commun.*, 2020, **56**, 13702.
4 B. Weber, W. Bauer and J. Obel, *Angew. Chem., Int. Ed.*, 2008, **47**, 10098.
5 K. Nishi, N. Matsumoto, S. Iijima, M. A. Halcrow, Y. Sunatsuki and M. Kojima, *Inorg. Chem.*, 2011, **50**, 11303.
6 B. Wever, W. Bauer, T. Pfaffeneder, M. M. Dîrtu, A. D. Naik, A. Rotaru and Y. Garcia, *Eur. J. Inorg. Chem.*, 2011, 3193.

7 I. Nemec, R. Herchel and Z. Trávníček, *Dalton Trans.*, 2015, **44**, 4474.
8 H. Oshio, H. Spiering, V. Ksenofontov, F. Renz and P. Gütlich, *Inorg. Chem.*, 2001, **40**, 1143.
9 C. A. Kilner and M. A. Halcrow, *Dalton Trans.*, 2010, **39**, 9008.
10 S. Hayami, Y. Komatsu, T. Shimizu, H. Kamihata and Y. H. Lee, *Coord. Chem. Rev.*, 2011, **255**, 1981.
11 F. Kobayashi, Y. Komatsumaru, R. Akiyoshi, M. Nakamura, Y. Zhang, L. F. Lindoy and S. Hayami, *Inorg. Chem.*, 2020, **59**, 16843.
12 A. B. Gaspar, M. C. Muñoz, V. Niel and J. A. Real, *Inorg. Chem.*, 2001, **40**, 9.
13 A. Galet, A. B. Gaspar, M. C. Muñoz and J. A. Real, *Inorg. Chem.*, 2006, **45**, 4413.
14 G. Agustí, C. Bartual, V. Martínez, F. J. Muñoz-Lara, A. B. Gaspar, M. C. Muñoz and J. A. Real, *New J. Chem.*, 2009, **33**, 1262.
15 S. Hayami, Y. Shigeyoshi, M. Akita, K. Inoue, K. Kato, K. Osaka, M. Tanaka, R. Kawajiri, T. Mitani and Y. Maeda, *Angew. Chem., Int. Ed.*, 2005, **44**, 4899.
16 S. Hayami, K. Murata, D. Urakami, Y. Kojima, M. Akita and K. Inoue, *Chem. Commun.*, 2008, 6510.
17 Y. Guo, X.-L. Yang, R.-J. Wei, L.-S. Zheng and J. Tao, *Inorg. Chem.*, 2015, **54**, 7670.
18 X. Zhang, H. Xie, M. Ballesteros-Rivas, Z.-X. Wang and K. R. Dunbar, *J. Mater. Chem. C*, 2015, **3**, 9292.
19 K. Takami, R. Ohtani, M. Nakamura, T. Kurogi, M. Sugimoto, L. F. Lindoy and S. Hayami, *Dalton Trans.*, 2015, **44**, 18354.
20 A. Ondo and T. Ishida, *Crystals*, 2018, **8**, 155.
21 M. Nakaya, R. Ohtani, J. W. Shin, M. Nakamura, L. F. Lindoy and S. Hayami, *Dalton Trans.*, 2018, **47**, 13809.
22 D. Shao, L. Shi, F.-X. Shen, X.-Q. Wei, O. Sato and X.-Y. Wang, *Inorg. Chem.*, 2019, **58**, 11589.
23 M. Nakaya, W. Kosaka, H. Miyasaka, Y. Komatsumaru, S. Kawaguchi, K. Sugimoto, Y. Zhang, M. Nakamura, L. F. Lindoy and S. Hayami, *Angew. Chem., Int. Ed.*, 2020, **59**, 10658.
24 H. E. Gottlieb, V. Kotlyar and A. Nudelman, *J. Org. Chem.*, 1997, **62**, 7512.
25 H. Yang, A. Z. Rys, C. K. McLaughlin and H. F. Sleiman, *Angew. Chem., Int. Ed.*, 2009, **48**, 9919.
26 G. M. Sheldrick, *Acta Crystallogr., Sect. A: Found. Adv.*, 2015, **71**, 3.
27 G. M. Sheldrick, *Acta Crystallogr., Sect. C: Struct. Chem.*, 2015, **71**, 3.
28 L. J. Bourhis, O. V. Dolomanov, R. J. Gildea, J. A. K. Howard and H. Puschmann, *Acta Crystallogr., Sect. A: Found. Adv.*, 2015, **71**, 59.
29 O. Kahn, *Molecular Magnetism*, VCH-Verlag, Weinheim, New York, 1993.
30 G. Yamamoto, C. Agawa, T. Ohno, M. Minoura and Y. Mazaki, *Bull. Chem. Soc. Jpn.*, 2003, **76**, 1801.
31 J. R. Malpass, P. S. Skerry and S. L. Rimmington, *Heterocycles*, 2004, **62**, 679.
32 J. K. Bjernemose and A. D. Bond, *Acta Crystallogr., Sect. E: Struct. Rep. Online*, 2004, **60**, o1143.
33 C. Berini, F. Minassian, N. Palloux-Léon, J.-N. Denis, Y. Vallée and C. Philouze, *Org. Biomol. Chem.*, 2008, **6**, 2574.
34 A. Okazawa, Y. Nagaichi, T. Nogami and T. Ishida, *Inorg. Chem.*, 2008, **47**, 8859.
35 P. A. Tziouris, C. G. Tsiafoulis, M. Vlasiou, H. N. Miras, M. P. Sigalas, A. D. Keramidas and T. A. Kabanos, *Inorg. Chem.*, 2014, **53**, 11404.
36 A. J. Kirby, J. E. Davies, T. A. S. Brandão, P. F. da Silva, W. R. Rocha and F. Nome, *J. Am. Chem. Soc.*, 2006, **128**, 12374.
37 A. Bondi, *J. Phys. Chem.*, 1964, **68**, 441.